Long-range excitons in conjugated polymers with ring torsions: poly( *para*-phenylene) and polyaniline



1998 J. Phys.: Condens. Matter 10 7679

(http://iopscience.iop.org/0953-8984/10/34/020)

J. Phys.: Condens. Matter **10** (1998) 7679–7690. Printed in the UK PII: S0953-8984(98)93157-5

# Long-range excitons in conjugated polymers with ring torsions: poly(*para*-phenylene) and polyaniline

Kikuo Harigaya†

Physical Science Division, Electrotechnical Laboratory, Umezono 1-1-4, Tsukuba 305-8568, Japan

Received 6 April 1998

**Abstract.** Ring torsion effects on the optical excitation properties of poly(*para*-phenylene) (PPP) and polyaniline (PAN) are investigated by extending the Shimoi–Abe model (Shimoi Y and Abe S 1996 *Synth. Met.* **78** 219). The model is solved using the intermediate-exciton formalism. Long-range excitons are characterized, and the long-range component of the oscillator strengths is calculated. We find that ring torsions affect the long-range excitons in PAN more readily than those in PPP, due to the larger torsion angle of PAN and the large number of bonds whose hopping integrals are modulated by torsions. Next, ring torsional disorder effects simulated by the Gaussian distribution function are analysed. The long-range component of the total oscillator strengths after sample averaging is nearly independent of the disorder strength in the PPP case, while that in the PAN case decreases readily as the disorder becomes stronger.

## 1. Introduction

Recently, we have been studying the structures of photoexcited states in electroluminescent conjugated polymers: poly(*para*-phenylene) (PPP), poly(*para*-phenylenevinylene) (PPV), poly(*para*-phenylenedivinylene) (PPD), and so on [1–3]. We have introduced the notion of long-range excitons in order to characterize photoexcited states in which an excited electron–hole pair is separated by more than the spatial extent of a single monomer of the polymer. We have shown [1, 2] that a long-range exciton feature starts at an energy on the higher-energy side of the lowest feature of the optical absorption of PPV. The presence of photoexcited states with large exciton radii is essential to the mechanisms of the strong photocurrents observed in this polymer. In reference [3], we compared the properties of excitons in PPV-related polymers. The oscillator strengths of the long-range excitons in PPP are smaller than those for PPV, and those for PPD are larger than those for PPV. Such relative variation is due to the difference in the number of vinylene bonds.

It is known that the PPV chain is nearly planar and that the phenyl rings are not distorted with respect to each other, as observed in x-ray analysis [4]. However, ring torsions, where even-number phenyl rings are rotated to the right around the polymer axis and odd-number phenyl rings are rotated to the left, have been observed in PPP [5]. The polymer structure of PPP is shown schematically in figure 1(a). The ring torsions originate from the steric repulsion between phenyl rings, because the distance between the neighbouring rings in PPP is smaller than that for PPV. In a simple tight-binding model, the ring torsion modulates the nearest-neighbour hopping integral $t$ as $t \cos \Psi$, where $\Psi$ is the torsion angle. If the angle $\Psi$

† E-mail: harigaya@etl.go.jp; URL: http://www.etl.go.jp/~harigaya/.

0953-8984/98/347679+12$19.50  

(a) PPP

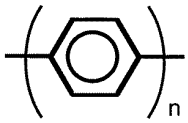


(b) PAN

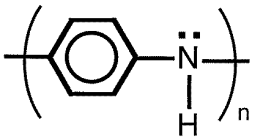


**Figure 1.** Polymer structures of (a) PPP and (b) PAN. These figures are only schematic. Geometries with ring torsions and the zigzag chain structure of PAN are used in the actual calculations.

was sufficiently large, the motion of electrons between phenyl rings would be hindered and also the exciton radius of the photoexcited states would become shorter. The contribution from long-range excitons will be smaller than that in the calculations [3] where a planar structure of PPP was assumed. The actual torsion angle of about 23° [5] may influence the results of the previous calculations. The first purpose of this paper is to examine ring torsion effects on optical excitations of PPP. We will show that the magnitude of the torsion, $\Psi \sim 23°$, does not change the component of the long-range excitons very much.

Another example of polymers in which ring torsions are present is polyaniline (PAN) (with a leucoemeraldine base). The schematic structure is displayed in figure 1(b). The phenyl rings and NH units are arrayed alternately in the chain direction. The magnitude of the torsion of the phenyl rings in PAN is about 56° [6]. This is larger than that for PPP, and thus the photoexcited states in PAN will be influenced more strongly by the torsion. In the last half of this paper, we shall look at this problem. We will show that the long-range component of the oscillator strengths at $\Psi = 56°$ has about half of the magnitude of that for the system without ring torsions. Long-range excitons in PAN are hindered by ring torsions more readily than those in PPP. This is due to the fact that the torsion angle is larger in PAN, and also because two bonds, whose hopping integrals are modulated as $t \cos \Psi$, are present between neighbouring phenyl rings in PAN while only one such bond is present between phenyls in PPP.

Furthermore, it is possible that the torsion angles in these polymers are not uniform throughout the systems. The torsion angles might fluctuate spatially owing to some perturbation effects with thermal origins or to external potentials. In this paper, such disorder effects are simulated by Gaussian distribution functions. The disorder strength is changed extensively, and the average long-range component is calculated for PPP and PAN. We show that the long-range component after sample averaging is nearly independent of the disorder strength in the PPP case, while that for the PAN case apparently decreases as the disorder becomes stronger.

This paper is organized as follows. In the next section, our model is described and the method of characterization of the long-range excitons is explained. In section 3, ring torsion effects on photoexcited states in PPP are reported. The results for PAN are given in section 4, and the paper is concluded with a summary in section 5.

## 2. Formalism

We consider optical excitations in PPP and PAN, by extending the Shimoi–Abe model [7] with electron–phonon and electron–electron interactions. The model is shown below:

$$H = H_{\rm pol} + H_{\rm int} \tag{1}$$

$$H_{\rm pol} = \sum_{i,\sigma} E_i c^{\dagger}_{i,\sigma} c_{i,\sigma} - \sum_{\langle i,j\rangle,\sigma} (t_{i,j} - \alpha y_{i,j})(c^{\dagger}_{i,\sigma} c_{j,\sigma} + \text{HC}) + \frac{K}{2} \sum_{\langle i,j\rangle} y^2_{i,j} \tag{2}$$

$$H_{\rm int} = U \sum_i \left( c^{\dagger}_{i,\uparrow} c_{i,\uparrow} - \frac{n_{\rm el}}{2} \right) \left( c^{\dagger}_{i,\downarrow} c_{i,\downarrow} - \frac{n_{\rm el}}{2} \right) + \sum_{i,j} W(r_{i,j}) \left( \sum_{\sigma} c^{\dagger}_{i,\sigma} c_{i,\sigma} - n_{\rm el} \right) \left( \sum_{\tau} c^{\dagger}_{j,\tau} c_{j,\tau} - n_{\rm el} \right). \tag{3}$$

In equation (1), the first term $H_{\rm pol}$ represents the tight-binding model along the polymer backbone with electron–phonon interactions which couple electrons with modulation modes of the bond lengths, and the second term $H_{\rm int}$ represents the Coulomb interaction potentials among the electrons. In equation (2), $E_i$ is the site energy at the $i$th site; $t_{i,j}$ is the hopping integral for hopping between the nearest-neighbour $i$th and $j$th sites in the ideal system without bond alternations; $\alpha$ is the electron–phonon coupling constant which modulates the hopping integral linearly with respect to the bond variable $y_{i,j}$ which measures the magnitude of the bond alternation of the bond $\langle i, j\rangle$ ($y_{i,j} > 0$ for longer bonds and $y_{i,j} < 0$ for shorter bonds (the average of $y_{i,j}$ is taken to be zero)); $K$ is the harmonic spring constant for $y_{i,j}$; and the sum is taken over the pairs of neighbouring atoms. Equation (3) describes the Coulomb interactions among the electrons. Here, $n_{\rm el}$ is the average number of electrons per site; $r_{i,j}$ is the distance between the $i$th and $j$th sites; and

$$W(r) = \frac{1}{\sqrt{(1/U)^2 + (r/aV)^2}} \tag{4}$$

is the parametrized Ohno potential. The quantity $W(0) = U$ is the strength of the on-site interaction; $V$ means the strength of the long-range part ($W(r) \sim aV/r$ in the limit $r \gg a$); and $a$ is the mean bond length.

The excitation wavefunctions of the electron–hole pair are calculated using the Hartree–Fock approximation followed by the single-excitation configuration interaction method. This method, which is appropriate for the cases of moderate Coulomb interactions—strengths between negligible and strong Coulomb interactions—is known as the intermediate-exciton theory in the literature [7, 8]. We write the singlet electron–hole excitations as

$$|\mu, \lambda\rangle = \frac{1}{\sqrt{2}} (c^{\dagger}_{\mu,\uparrow} c_{\lambda,\uparrow} + c^{\dagger}_{\mu,\downarrow} c_{\lambda,\downarrow}) |g\rangle \tag{5}$$

where $\mu$ and $\lambda$ stand for unoccupied and occupied states, respectively, and $|g\rangle$ is the Hartree–Fock ground state. The general expression of the $\kappa$th optical excitation is

$$|\kappa\rangle = \sum_{(\mu,\lambda)} D_{\kappa,(\mu,\lambda)} |\mu, \lambda\rangle. \tag{6}$$

After inserting this relation together with the site representation $c_{\mu,\sigma} = \sum_i \alpha_{\mu,i} c_{i,\sigma}$, we obtain

$$|\kappa\rangle = \frac{1}{\sqrt{2}} \sum_{(i,j)} B_{\kappa,(i,j)} (c^{\dagger}_{i,\uparrow} c_{j,\uparrow} + c^{\dagger}_{i,\downarrow} c_{j,\downarrow}) |g\rangle \tag{7}$$

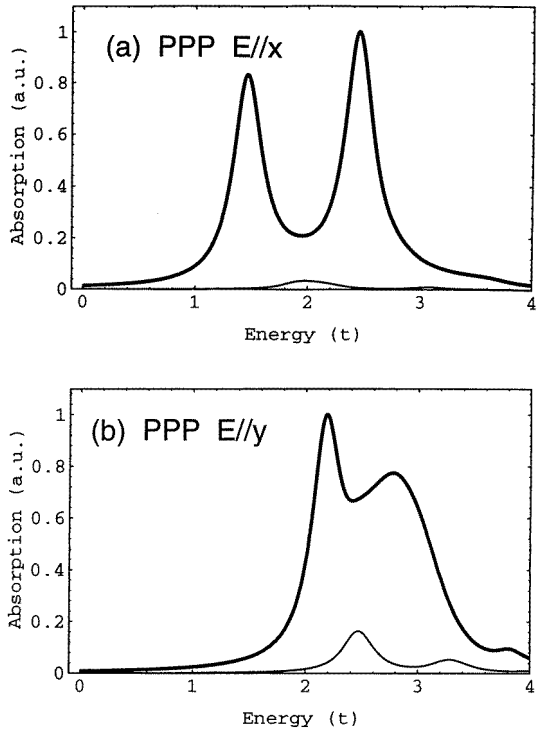


**Figure 2.** Optical absorption spectra of PPP shown in arbitrary units. The polymer axis is parallel to the $x$-axis. The polymer without ring torsions is in the $x$–$z$ plane. The electric field of the light is parallel to the chain and in the direction of the $x$-axis in (a), and it is perpendicular to the chain and along the direction of the $y$-axis in (b). It is along the direction of the $z$-axis in (c). The orientationally averaged spectra are shown in (d). The number of PPP monomer units is $N_{\rm m} = 20$. The bold line represents the total absorption. The thin line indicates the absorption of the long-range component. The Lorentzian broadening $\gamma = 0.15\ t$ is used.

where

$$B_{\kappa,(i,j)} = \sum_{(\mu,\lambda)} D_{\kappa,(\mu,\lambda)} \alpha^{*}_{\mu,i} \alpha_{\lambda,j}. \tag{8}$$

Thus, $|B_{\kappa,(i,j)}|^2$ is the probability that an electron locates at the $i$th site and a hole is at the $j$th site.

We shall define the following quantity:

$$P_{\kappa} = \sum_{i \in M} \sum_{j \in M} |B_{\kappa,(i,j)}|^2 \tag{9}$$

where $M$ is a set of sites within a single monomer—in other words, a set of carbon sites included in the brackets of each polymer shown in figure 1. When $P_{\kappa} > 1/N_{\rm m}$ ($N_{\rm m}$ is the number of monomers used in the calculation of periodic polymer chains), the electron and hole favour having large amplitudes in the same single monomer. Then, this excited state is identified as a short-range exciton. On the other hand, when $P_{\kappa} < 1/N_{\rm m}$, the excited state is characterized as a long-range exciton. This characterization method is performed for all of the photoexcited states $|\kappa\rangle$, and a long-range component in the optical absorption spectrum is extracted from the total absorption.

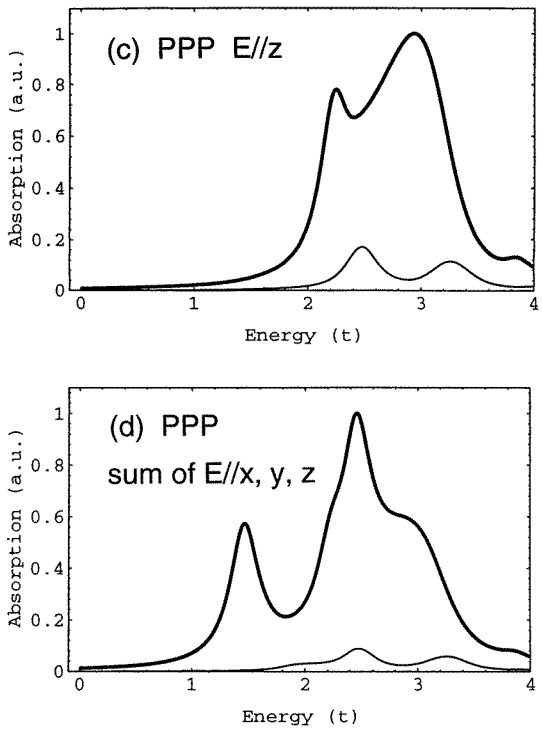


**Figure 2.** (Continued)

## 3. PPP

### *3.1. Ring torsion effects*

In this section, the torsion angle between neighbouring phenyl rings $\Psi$ is taken into account in the hopping integral without ring torsions by substituting $t - \alpha y \Rightarrow (t - \alpha y)\cos\Psi$ in the model reviewed above. Here, $y$ is the length change of the corresponding bond. The parameter values used in this section are $\alpha = 2.59\ t$ Å$^{-1}$, $K = 26.6\ t$ Å$^{-2}$, $U = 2.5\ t$, and $V = 1.3\ t$. They have been determined by comparison with experiments on PPV [7], and have been used in [1, 8]. Most of the quantities in energy units are indicated by being given in units of $t$ in this paper. The model is solved by using the mean-field approximation, and electron–hole excitations are calculated using the intermediate-exciton formalism. The long-range component of the photoexcited states is characterized as we have indicated in the previous section.

Figure 2 shows the optical absorption spectra calculated for the system with the torsion angle $\Psi = 23^\circ$ [5] and the monomer number $N_m = 20$. The spectral shapes are nearly independent of the monomer number at $N_m = 20$, as reported in [3]. The polymer without ring torsions with an open boundary is in the $x$–$z$ plane. The electric field of the light is parallel to the chain and in the direction of the $x$-axis in figure 2(a), and it is perpendicular to the chain and is in the direction of the $y$-axis in figure 2(b). The electric field is in the direction of the $z$-axis in figure 2(c). The spectra averaged orientationally with respect to the electric field are shown in figure 2(d). In each figure, the bold line shows the total absorption and the thin line shows the contribution from the long-range excitons for

the case where the photoexcited electron and hole are separated by more than the spatial extent of a single monomer. In figure 2(a), there are two main features at around 1.4 $t$ and 2.4 $t$, where quantities with energy dimensions are expressed in units of $t$. There is a long-range-exciton feature at around $\sim$2.0 $t$ on the higher-energy side of the 1.4 $t$ main peak. In contrast, the 2.4 $t$ feature does not have so strong a long-range component due to the almost localized nature of the excitons. This is similar to the case for the calculations in [3], and the ring torsions do not change the almost localized character of the feature at around 2.4 $t$ [9]. Figure 2(b) shows the case where the electric field is parallel to the $y$-axis. If the ring torsions are not present, the oscillator strengths are zero in this case. However, they are finite, and the maximum of the bold line in figure 2(b) is one order of magnitude smaller than that for figure 2(a). Two main features of the energies of 2.2 $t$ and 2.8 $t$ are derived from those of the case with the electric field in the $z$-direction, shown in figure 2(c). These features in figure 2(c) contribute dominantly, and their oscillator strengths are of the same order of magnitude as those of figure 2(a). There are long-range components of these two features around the energies of about 2.5 $t$ and 3.3 $t$. Figure 2(d) shows the optical spectra for the case where the electric field is orientationally averaged. The overall spectral shape is similar to that in the case without ring torsions, with $\Psi = 0$ [3]. However, the spectral width decreases slightly due to the smaller hopping interactions between neighbouring phenyl rings.

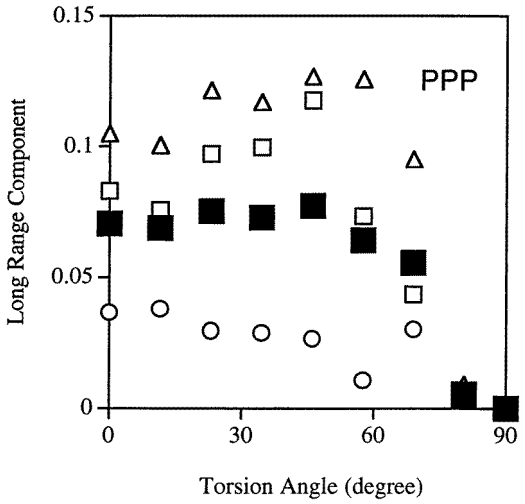


**Figure 3.** The long-range component of the optical absorption spectra as a function of the torsion angle in PPP. The monomer unit number is $N_m = 20$. The closed squares are for the orientationally averaged absorption. The open circles, squares, and triangles indicate the data for the cases with the electric field parallel to the $x$-, $y$-, and $z$-axes, respectively.

Next, we vary the torsion angle $\Psi$ in the Hamiltonian, and look at the changes in the optical spectra. We calculate the long-range component in the total oscillator strengths, as we have done in [1–3]. We search for its variations as a function of $\Psi$. Figure 3 shows the calculated results. The closed squares show the data for the orientationally averaged absorption. The open circles, squares, and triangles indicate the data for the cases with the electric field parallel to the $x$-, $y$-, and $z$-axes, respectively. We find that the average long-range component depends weakly on $\Psi$ up to a magnitude of $\Psi$ of about 40°. Thus, we have examined ring torsion effects on optical excitations of PPP. We have found that

the magnitude of the torsion, $\Psi \sim 23^\circ$, does not change the component of the long-range excitons very much from that of the torsion-free system. However, the long-range component suddenly deceases at larger $\Psi$, and becomes zero at $\Psi = 90^\circ$. This is a natural result of the broken conjugations due to strong ring torsions. The long-range components with the field in the $y$- and $z$-directions are generally larger than that of the $x$-direction case. This property has been seen in reference [3], too.

### *3.2. Torsional disorder*

Ring torsional disorder effects are taken into account by the Gaussian distribution function with the standard deviation $\delta\Psi$. This quantity is varied within the range $0^\circ \leqslant \delta\Psi \leqslant 90^\circ$. In this subsection, we report the results averaged over 1000 samples of Gaussian disorder for the system with $N_m = 10$. This value of $N_m$ is half of that of the previous subsection; this change was made in order to allow us to spend more numerical calculation time taking sample averages to give the distribution of the disorder.

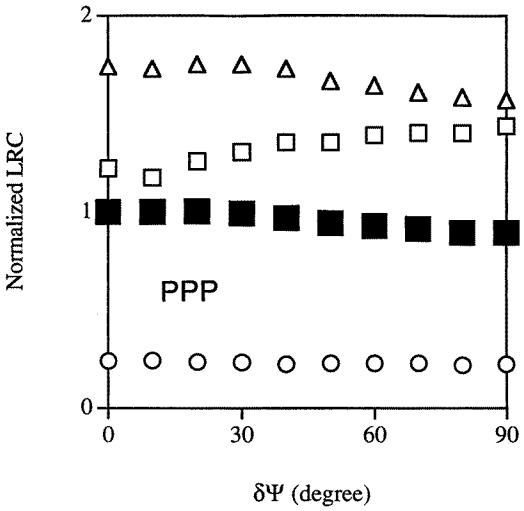


**Figure 4.** The long-range component (LRC) of the optical absorption spectra as a function of the torsional disorder strength $\delta\Psi$ in PPP with $\Psi$ fixed as $23^\circ$. The monomer unit number is $N_m = 10$, and the number of disordered samples is 1000. The closed squares are for the orientationally averaged absorption. The open circles, squares, and triangles indicate the data for the cases with the electric field parallel to the $x$-, $y$-, and $z$-axes, respectively. The left-hand axis is normalized with respect to the LRC of the orientationally averaged absorption in the system without disorder.

Figure 4 shows the sample-averaged long-range component (LRC) against the disorder strength $\delta\Psi$. The static torsion angle—in other words, the torsion angle of the system without disorder—is fixed as $\Psi = 23^\circ$. The left-hand axis is scaled with respect to the LRC of the orientationally averaged absorption in the system without disorder. The closed squares are for the orientationally averaged absorption. Therefore, this quantity is unity at $\delta\Psi = 0$. The open circles, squares, and triangles indicate the data for the cases with the electric field parallel to the $x$-, $y$-, and $z$-axes, respectively. The data with the electric field parallel to the $y$-axis are smaller than the orientationally averaged data. Those for cases with the electric field parallel to the $x$- and $z$-axes are larger than the data shown by the

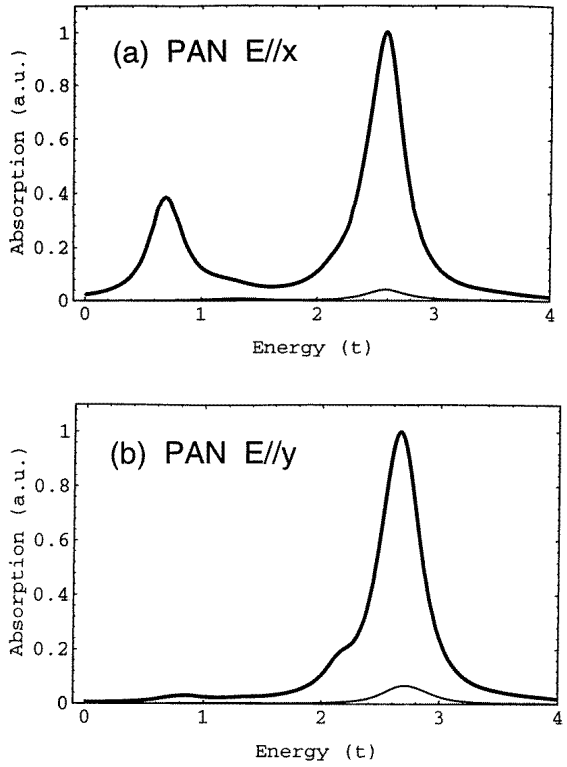


**Figure 5.** Optical absorption spectra of PAN shown in arbitrary units. The polymer axis is parallel to the $x$-axis. The polymer without ring torsions is in the $x$–$z$ plane. The electric field of the light is parallel to the chain and in the direction of the $x$-axis in (a), and it is perpendicular to the chain and is in the direction of the $y$-axis in (b). It is in the direction of the $z$-axis in (c). The orientationally averaged spectra are shown in (d). The number of PAN monomer units is $N_{\mathrm{m}} = 20$. The bold line represents the total absorption. The thin line indicates the absorption of the long-range component. The Lorentzian broadening $\gamma = 0.15\ t$ is used.

closed squares. The most important result is that the dependence of the LRC on $\delta\Psi$ is very weak. The LRC does not change very much even if $\delta\Psi$ increases to as much as 90°. This indicates that the long-range excitons survive in the face of extra perturbations by the torsional disorder.

## 4. PAN

### *4.1. Ring torsion effects*

It is of some interest to investigate ring torsion effects in conjugated polymers for which the torsion angles are larger than that of PPP. In this section, we look at torsion effects in PAN as a typical example of such polymers. The polymer structure is shown schematically in figure 1(b). The zigzag geometry of PAN is taken into account in the actual calculations, even though it is not shown in figure 1(b). For model parameters, we have assumed the negative site energy $E_{\mathrm{N}} = -0.571\ t$ at the N sites ($E_{\mathrm{C}} = 0$ at the C sites), the hopping integral $t_{\mathrm{C-N}} = 0.8\ t$ between carbon and nitrogen ($t_{\mathrm{C-C}} = t$ as in PPP), the on-site

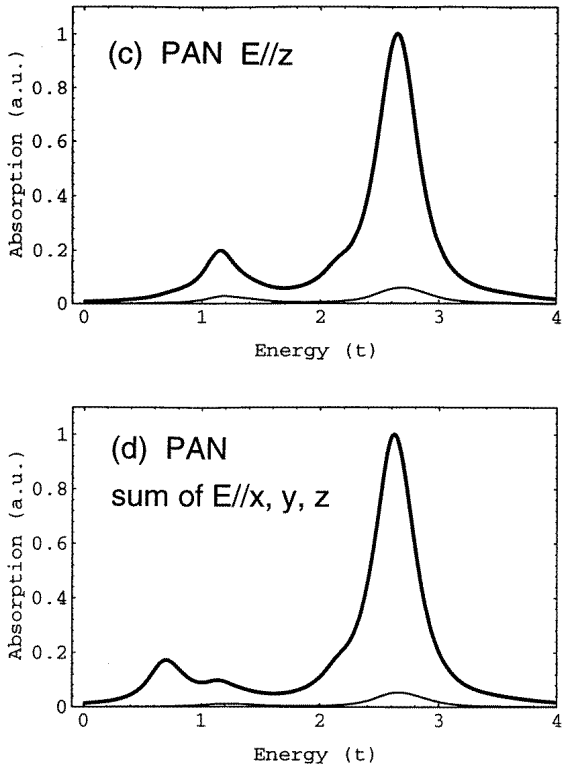


**Figure 5.** (Continued)

interaction strength $U = 2\ t$, and the magnitude of long-range interactions $V = 1\ t$. The parameters $E_{\mathrm{N}}$ and $t_{\mathrm{C-N}}$ are taken from [10] as representative values. We show the results for the monomer number $N_{\mathrm{m}} = 20$. We have taken several combinations of Coulomb interaction parameters and have looked at the changes of the results. We have found that the long-range component as a function of $\Psi$ depends weakly on $U$ and $V$. Thus, we report the results for just one combination of Coulomb parameters.

Figure 5 shows the calculated optical absorption spectra of PAN with the torsion angle $\Psi = 56^{\circ}$. The three-dimensional coordinates of the polymer are similar to those of PPP in figure 2. In figure 5(a), the electric field is along the direction of the polymer axis, and is in the $x$-direction. There are two main features at around 0.6 $t$ and 2.6 $t$. The former has a smaller long-range exciton feature than the latter. As we observe in the band structure of PAN [10], the lowest optical excitation between the valence band and the conduction band has a certain magnitude of dispersions, and thus its long-range component might be observed. However, this lowest exciton is dipole forbidden in the system without ring torsions when the electric field is parallel to the chain direction. There is the second-lowest optical excitation, which is almost localized and is dipole allowed in the system without torsions, at the excitation energy near that of the lowest exciton. Thus, the long-range component of the 0.6 $t$ feature is suppressed. Figure 5(b) shows the weak optical absorption originating from the finite torsions which we have discussed for PPP; see figure 2(b). Figure 5(c) shows the optical spectra obtained when the electric field is in the $z$-direction. Two features at around 1.2 $t$ and 2.6 $t$ have certain magnitudes of oscillator strengths due to

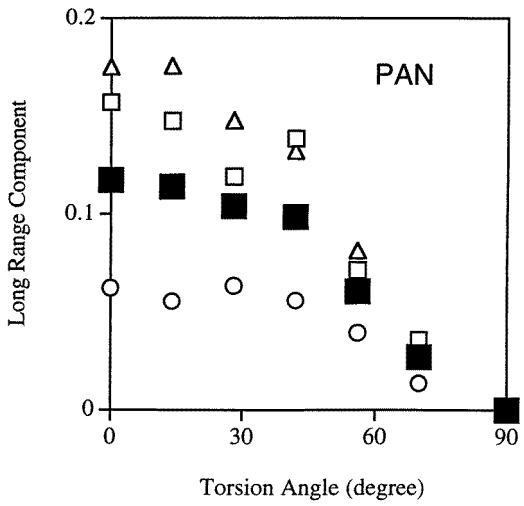


**Figure 6.** The long-range component of the optical absorption spectra as a function of the torsion angle in PAN. The monomer unit number is $N_m = 20$. The closed squares are for the orientationally averaged absorption. The open circles, squares, and triangles indicate the data for the cases with the electric field parallel to the $x$-, $y$-, and $z$-axes, respectively.

long-range excitons. This qualitative property is similar to that shown in figure 2(c). Then, figure 5(d) shows the optical spectra obtained when orientational averaging is performed. We find that excitation features can be understood by superposing those of figures 5(a), 5(b), and 5(c).

Next, we show the long-range component of the oscillator strength as a function of the torsion angle $\Psi$ in figure 6. In contrast to the case for PPP, the long-range component decreases smoothly as $\Psi$ increases. The long-range component of the total oscillator strengths at the observed value $\Psi = 56^\circ$ has about half of the magnitude of that for the system without ring torsions. Thus, the long-range excitons in PAN can be hindered by ring torsions more readily than those in PPP. This is due to the fact that the torsion angle is larger in PAN, and also that two bonds, whose hopping integrals are modulated as $t \cos\Psi$, are present between neighbouring phenyl rings in PAN while just one such bond is present between phenyls in PPP.

### *4.2. Torsional disorder*

Ring torsional disorder effects are studied for PAN using the Gaussian distribution function with the standard deviation $\delta\Psi$ which is varied within the range $0^\circ \leqslant \delta\Psi \leqslant 90^\circ$. The number of disordered samples is 1000, and $N_m = 10$ in this subsection.

Figure 7 shows the sample-averaged LRC as a function of the disorder strength $\delta\Psi$. The torsion angle of the system without disorder is fixed as $\Psi = 56^\circ$. The left-hand axis is normalized as was done for PPP in figure 4. The closed squares are for the orientationally averaged absorption. The open circles, squares, and triangles indicate the data for the cases with the electric field parallel to the $x$-, $y$-, and $z$-axes, respectively. The magnitudes of the four quantities at $\delta\Psi = 30^\circ$ are about half of the magnitudes at $\delta\Psi = 0$. Therefore, the LRC of PAN is hindered by the torsional disorder more readily than that of PPP. Such a remarkable contrast between PPP and PAN is similar to the contrast of the static torsion

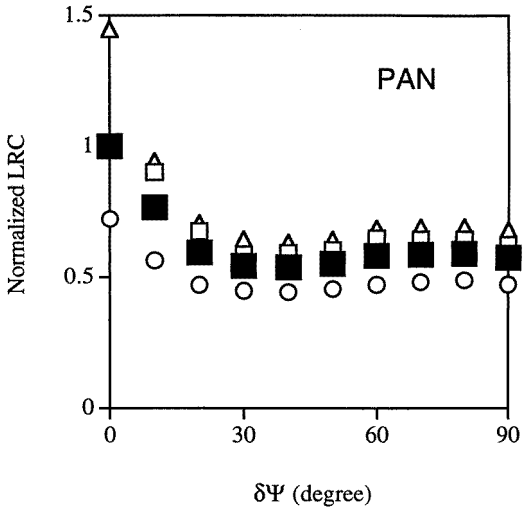


**Figure 7.** The long-range component (LRC) of the optical absorption spectra as a function of the torsional disorder strength $\delta\Psi$ in PAN with $\Psi$ fixed at 56°. The monomer unit number is $N_m = 10$, and the number of disordered samples is 1000. The closed squares are for the orientationally averaged absorption. The open circles, squares, and triangles indicate the data for the cases with the electric field parallel to the $x$-, $y$-, and $z$-axes, respectively. The left-hand axis is normalized with respect to the LRC of the orientationally averaged absorption in the system without disorder.

angle effects which we discussed in the previous subsection. Thus, we have found that the spatial extent of excitons in PAN is readily limited by torsional disorder as well as by static ring torsions.

## 5. Summary

We have examined the ring torsion effects which might hinder delocalization of excitons in the chain direction of the conjugated polymers PPP and PAN. Long-range excitons in the optical excitations have been characterized, and the long-range component of the oscillator strengths has been calculated as a function of the torsion angle. We have shown that the torsion effects in PPP are relatively small. In contrast, the torsions of PAN decrease the magnitude of the long-range component to about half of its value for the torsion-free system. Next, ring torsional disorder effects simulated by a Gaussian distribution function have been analysed. The long-range component of the total oscillator strengths after sample averaging is nearly independent of the disorder strength $\delta\Psi$ in the PPP case, while that for PAN decreases readily as $\delta\Psi$ becomes stronger.

## Acknowledgments

Useful discussions with Y Shimoi, S Abe, and K Murata are acknowledged. The numerical calculations were performed on the DEC AlphaServer of the Research Information Processing System Centre (RIPS), Agency of Industrial Science and Technology (AIST), Japan.

## References

[1] Harigaya K 1997 *J. Phys. Soc. Japan* **66** 1272
[2] Harigaya K 1997 *J. Phys.: Condens. Matter* **9** 5253
[3] Harigaya K 1997 *J. Phys.: Condens. Matter* **9** 5989
[4] Chen D, Winokur M J, Masse M A and Karasz F E 1990 *Phys. Rev.* B **41** 6759
[5] Baudour J L, Delugeard Y and Rivet P 1978 *Acta Crystallogr.* B **34** 625
[6] Jozefowicz M E, Laversanne R, Javadi H H S, Epstein A J, Pouget J P, Tang X and MacDiarmid A G 1989 *Phys. Rev.* B **39** 12 958
[7] Shimoi Y and Abe S 1996 *Synth. Met.* **78** 219
[8] Harigaya K, Shimoi Y and Abe S 1996 *Proc. 2nd Asia Symp. on Condensed Matter Phytophysics (Konan University, Kobe)* p 25
[9] Soos Z G, Etemad S, Galvão D S and Ramasesha S 1992 *Chem. Phys. Lett.* **194** 341
[10] Ginder J M and Epstein A J 1990 *Phys. Rev.* B **41** 10 674